



Mechanism study of the electrical discharge ablation milling with a microcutting depth

Yunxiao Han¹ · Zhidong Liu¹ · Qingcai Chen¹ · Mingbo Qiu¹ · Hongpeng Mu¹

Received: 3 November 2020 / Accepted: 19 January 2021 / Published online: 11 February 2021
© Springer-Verlag London Ltd., part of Springer Nature 2021

Abstract

Tool wear inevitably occurs during electrical discharge milling (ED milling), adversely affecting the form precision of machined features. Specifically, radial tool wear negatively influences copying precision. In this study, electrical discharge ablation milling (EDA milling) with a microcutting depth was investigated to improve the machining precision of discharge milling. In the proposed method, the cutting depth of a single layer was kept at the micron level, which is smaller than the discharge gap, and the electrode was set to a fast feeding rate at a constant speed. The microcutting depth of a single layer made the discharge concentrate at the end of the electrode while avoiding the side. Under this method, radial tool wear is prevented to realize high-precision discharge milling. The discharge state and high-precision mechanism of the proposed method were analyzed. Contrast experiments were conducted to compare conventional electrical discharge milling (ED milling), conventional electrical discharge ablation milling with a large cutting depth (EDA milling with a large cutting depth), and EDA milling with a microcutting depth. Results indicated that when peak current was 30A (pulse duration was 150 μ s and pulse interval was 120 μ s), the machining efficiency of the proposed method (18.8 mm³/min) was 9.5 times that of ED milling (1.97 mm³/min) and was 62% higher than that of EDA milling with a large cutting depth (11.6 mm³/min). Besides, the surface quality and cross-sectional shape precision of the straight groove were significantly improved compared with EDA milling with a large cutting depth.

Keywords Electrical discharge machining (EDM) · Microcutting depth · Rapid feed · Electrical discharge ablation milling (EDA milling) · High precision

1 Introduction

Electrical discharge milling (EDM) is a suitable method for machining complex geometric shapes and difficult-to-cut materials by conventional mechanical processing [1]. The approach is widely applied in aerospace, military, automotive, instrumentation, medical equipment, and micro-machinery manufacturing fields [2].

Thermoelectric heating during EDM can erode electrodes, resulting in tool wear, which directly affects machining precision [3]. The ratio of the electrode discharge area to the machining surface area in ED milling is considerably smaller than that in die-sinker EDM. Thus, tool wear exerts an

increased impact on machining precision when the tool wear rate is the same. Numerous local and foreign studies have been conducted on the tool wear of EDM over the years.

To determine the mechanism of tool wear, Mohri et al. [4] conducted a study on the change in electrode shape over time by online measurement. Kunieda and Kobayashi [5] employed spectroscopy to measure the rate of tool wear during EDM by detecting the electrode material vaporization density. Tool wear was reduced by prolonging the discharge time, which was conducive to depositing a thickened carbon film on the electrode surface, effectively preventing tool wear. Cheong et al. [6] pointed that the reverse current caused by oscillation when using an RC circuit worsened the relative wear ratio of the tool. Wang et al. [7] proposed a method to analyze a reverse current flow in micro-EDM process during the counting and monitoring of pulses in order to reduce the tool electrode wear. For the prediction modeling of tool wear, Bissacco et al. [8] estimated tool wear on the basis of the amount of the workpiece material removed per discharge and verified its reliability. Zarepour et al. [9] established a

✉ Zhidong Liu
liutim@nuaa.edu.cn

¹ College of Mechanical and Electrical Engineering, Nanjing University of Aeronautics and Astronautics, Nanjing 210016, China

prediction model by regression analysis and obtained the optimal factor level. Zhang et al. [10] performed a two-dimensional geometric simulation of a cylindrical electrode for micro-EDM to explain and predict the formation of tapered electrodes, which was used to optimize compensation parameters to avoid insufficient or excessive compensation. Pei et al. [11] subsequently proposed a tool wear model based on electromagnetic field theory. This model predicted the discharge area by replacing the distance between the electrodes with the intensity of the electric field, and the prediction was more accurate. The method to compensate for tool wear to improve the precision of EDM has also been studied. Bleys et al. [12] compensated tool wear in real time by using sensors; simulation and experiments were then conducted by Bleys et al. [13] for verification. Bellotti et al. [14] developed an adaptive tool wear compensation strategy by combining traditional linear compensation method and tool wear sensing, and the method was validated for an industrially relevant case. Yu et al. [15] proposed a method for the uniform compensation of micro-EDM tool wear, adopted layer-by-layer processing, and performed quantitative feed compensation for each layer through the Z axis, ultimately achieving complex workpiece processing. On the basis of the aforementioned study, Yu et al. [16] proposed a method combining linear compensation and uniform consumption and then established a theoretical model. Experimental results showed a reduction in tool wear. Liang et al. [17] proposed a self-repair method and a profile error compensation method of the tool electrode wear to improve the processing accuracy. The self-repair method was to plan and control the rotation motion of the tool electrode for maintaining its shape. The profile error compensation method was to modify the Z coordinate of the tool electrode for decreasing the machining error. Li et al. [18] found that the actual erosion depth was collectively determined by discharge energy, layer thickness and scanning speed. They proposed scanning speed adjusted with layer (SSAL) strategy based on the established mathematical model of erosion depth and the depth error was reduced in layer-by-layer micro-EDM.

Previous research has identified certain advantages, but there are still disadvantages. Electrical discharge milling used to be strongly affected by high-speed milling because of low efficiency. This problem has recently been solved and considerable potential in aerospace and mold manufacturing with the proposed of Blue-Arc technology, combined high-speed EDM milling and arc machining [19], blasting erosion arc machining [20], electrical discharge ablation machining [21], and combined machining technology [22]. However, most studies on tool wear have focused on micro-EDM; research on tool wear in conventional size discharge milling has rarely been reported. Second, tool wear in discharge milling includes end wear and side wear, as shown in Fig. 1. End wear reduces the axial length of the electrode, affecting the dimensional accuracy of machining. Side wear leads to a change in

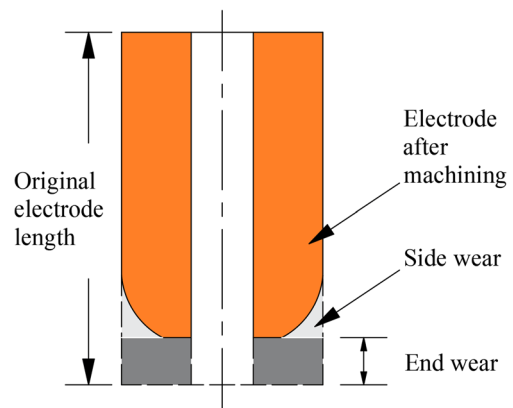


Fig. 1 The different kinds of tool wear

electrode shape, mainly influencing the shape precision of machining. Even with the application of compensation technology, which has been proposed in earlier reports, it can only compensate for end wear in conventional size ED milling; the lower shape precision caused by side wear cannot be solved.

In this study, a hollow porous copper electrode was used to perform EDA milling with microcutting depth technology. The proposed method has two characteristics: ① The cutting depth of a single layer was set smaller than the discharge gap, which could not be realized in conventional ED milling. ② The electrode was set to a fast feeding rate at a constant speed during whole processing, which was obviously different from the servo feed of electrode according to the state between electrodes in conventional ED milling. The efficiency of the proposed method was increased exponentially relative to that of conventional ED milling. Radial tool wear caused by side discharge during conventional EDA milling with a large cutting depth was overcome by the proposed technology, and copying precision was greatly improved.

2 Design of the experiment

2.1 Basic principle of EDA milling with a microcutting depth

To evaluate the cutting depth parameters under EDA milling with a microcutting depth, the manual feeding and hover functions of the EDM tool were used to detect the discharge gap of EDA milling under the following experimental conditions: peak current, 15 A; pulse duration, 150 μ s; pulse interval, 120 μ s; oxygen pressure, 0.25 MPa; water pressure, 0.23 MPa. The measurement method was as follows: ① For tool setting, the Z-coordinate was cleared. ② The electrode was pulled to 120 μ m from the zero point of the Z axis. ③ The hover mode was selected, the pulse power supply was turned on, and the feed speed was adjusted to the micron level. The electrode was manually fed until normal discharge was

observed (as determined from the discharge voltage waveform displayed by the oscilloscope and the discharge frequency displayed by the pulse counter). ④ The pulse power supply was turned on, and the Z axis value at this time was recorded. The absolute value of the Z axis was considered as the discharge gap under the parameter. Measurement was conducted 10 times, and the average measurement was used to determine the discharge gap (26 μm).

The cutting depth of a single layer under EDA milling with a microcutting depth was controlled at the micron level to ensure that it was smaller than the discharge gap (26 μm). Thus, the electrode was suspended above the workpiece during machining. The risk of a side wall collision between the electrode and the workpiece was then avoided. After a large number of experimental trials, in this study, the cutting depth of a single layer of 10 μm was used under EDA milling with a microcutting depth. The electrode was set to a fast feeding rate at a constant speed (after multiple trials in the early stage, maximum machining efficiency was achieved under the following conditions: cutting depth of a single layer, 10 μm ; constant feed rate, 10 mm/s; no continuous short-circuit during stable machining for 60 min). Simultaneously, the high-pressure mixed aerosol dielectric of water and oxygen entered the machining area through the inside of the hollow electrode. The spark discharge was concentrated toward the end face of the electrode. The discharge point of the metal material reached the ignition point under high-temperature spark discharge. Intense oxidized combustion reaction occurred between the molten metal and oxygen, which effectively ablated the workpiece material. The relationship between the cutting depth of the single-layer l and the discharge gap D is illustrated in Fig. 2.

2.2 Experimental setup

The experimental system is presented in Fig. 3 in accordance with the basic principle described in a previous section. During the process, high-pressure oxygen and high-pressure

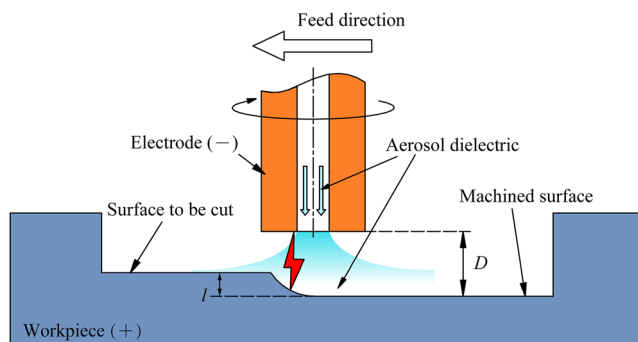


Fig. 2 Relationship between the cutting depth of single-layer l and the discharge gap D

water flow continuously into the atomizing nozzle and are mixed inside the nozzle to form aerosol dielectric, which is injected into the machining area via the hollow electrode. The atomizing device and electrode are fixed on the spindle of the machine tool. The electrode is a round hollow porous copper electrode with an outer diameter of 3 mm. A data acquisition unit is used to record and analyze the discharge waveform.

2.3 Experiment content and parameters

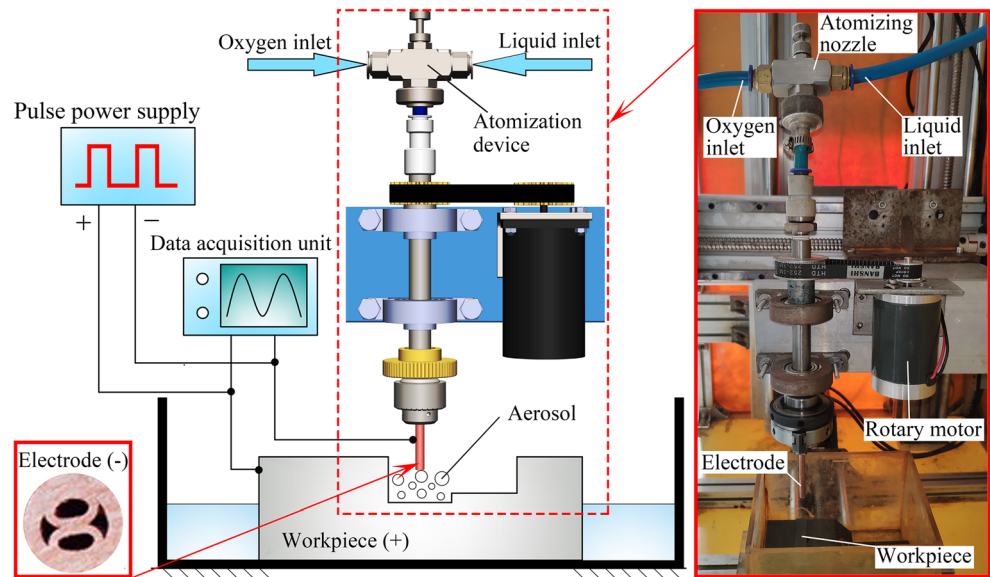
Conventional ED milling, EDA milling with a large cutting depth, and EDA milling with a microcutting depth were used to machine the straight groove under similar experimental conditions to verify the superiority of EDA milling with a microcutting depth to the other techniques. The cutting depth of a single layer under ED milling was set to 0.3 mm and that under EDA milling with a large cutting depth was set to 1 mm for high-efficiency EDA milling. The electrode feed (X direction) under these two methods was servo-fed by average voltage detection. Under EDA milling with a microcutting depth, the cutting depth of a single layer was set to 10 μm , and the electrode was suspended above the workpiece at a fast speed (constant at 10 mm/s). The experimental parameters are listed in Table 1.

3 Mechanism of EDA milling with a microcutting depth

3.1 Discharge state

The waveforms recorded by the data acquisition unit were analyzed to obtain the discharge waveform composition of two types of EDA milling, as shown in Fig. 4. EDA milling with a microcutting depth includes three types of discharge states: discharge ablation state, short-circuit state, and open-circuit state. The discharge ablation state was a normal processing state, comprising 56%. The workpiece material was quickly removed in this state. During the electrode fast feeding process, the thickness of the ablated material was greater than the cutting depth of the single-layer l (Fig. 5). When the level of energy was too high, there was a high probability of an open-circuit state when the next layer was milled here. From the above section, ablation reaction formed a large amount of energy; thus, the frequency of this occurrence was considerably high, resulting in an open-circuit state, which comprised 42%. Moreover, the electrode was suspended above the workpiece because the discharge gap was greater than the cutting depth of the single layer. Ideally, no short-circuit should occur during processing. However, in actual processing, the huge ablation energy produced large-scale ablation products, which passed between the workpiece and the electrode during removal, and a short

Fig. 3 Details of the experimental setup



circuit occurred at the overlap joint of both ends of the electrode, as shown in state A (dashed line in Fig. 6). The electrode and workpiece were staggered away from each other quickly (state B in Fig. 6) because of the rotation and fast feed of the electrode; thus, the short-circuit state between the electrodes was brief.

The short-circuit state rate of EDA milling with a large cutting depth was 22%. By contrast, EDA milling with a microcutting depth had a short-circuit rate of only 2% because of the small cutting depth and short-circuit self-recovery (shown in red in Fig. 4). EDA milling with a microcutting depth substantially reduced the state of short-circuit and

unstable discharge and increased the probability of normal discharge (shown in dark green in Fig. 4), improving the utilization rate of ablation energy and greatly improving the machining efficiency.

3.2 Mechanism of high precision

The cutting depth of the single layer was larger than the discharge gap under EDA milling with a large cutting depth and conventional ED milling. Thus, spark discharges occurred at the end and sides of the electrode. The discharge position diagram of EDA milling with a large cutting depth is

Table 1 Experimental parameters

Items	EDA milling with a microcutting depth	EDA milling with a large cutting depth	ED milling
Workpiece	Hardening die steel Cr12; density 7.87 g/mm ³		
Pulse parameters	Pulse duration: Pulse interval = 150 μs:120 μs		
Current	30A		
Polarity	Positive polarity (workpiece is connected to the anode)		
Machining depth	2 mm		
Electrode	Hollow porous copper tube electrode; density 8.9 g/mm ³ ; outer diameter 3 mm; rotating speed 150 r/min		
Water parameters	0.23 MPa; continuous supply		
Gas parameters	Industrial oxygen (purity 99.5%); pressure 0.25 MPa; continuous supply	Industrial oxygen (purity 99.5%); pressure 0.25 MPa; continuous supply	No gas
Cutting depth of single layer	10 μm	1 mm	0.3 mm
Electrode feed	10 mm/s constant speed feed	Servo feed with average voltage detection	Servo feed with average voltage detection

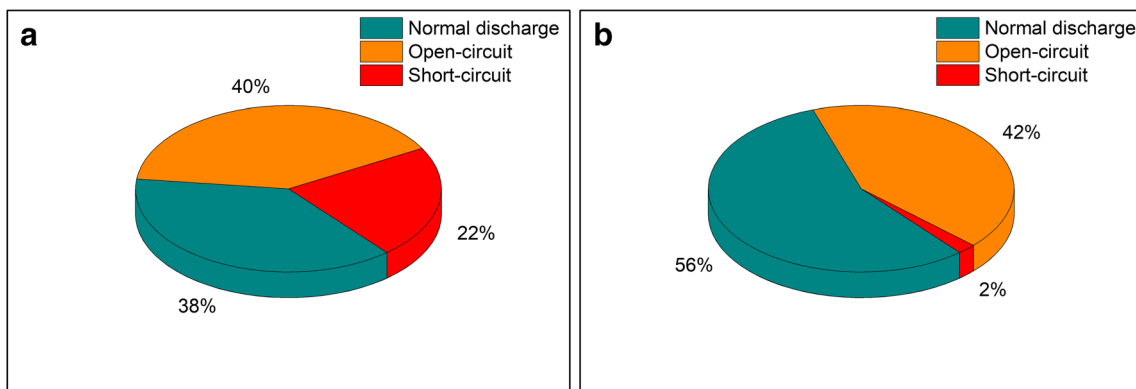


Fig. 4 Proportion of discharge state. a EDA milling with a large cutting depth. b EDA milling with a microcutting depth

presented in Fig. 7a. Side discharge was the primary means of removing the material, resulting in substantial tool wear along the side of the electrode. Large non-uniform loss formed round corners at the electrode end (Fig. 8a and b). The shape precision was affected, and the desired processing effect was not achieved. Moreover, compensating for the tool was extremely difficult because of the non-uniformity of tool wear. For EDA milling with a microcutting depth, the cutting depth of a single layer was less than the discharge gap; thus, tool wear mainly occurred at the end of the electrode. The shape of the electrode remained cylindrical (Fig. 8c). Shape precision of the machined groove was ensured.

4 Results and discussion

4.1 Analysis of MRR

The MRRs achieved using the three processing methods are presented in Fig. 9. EDA milling with a microcutting depth exhibited the highest MRR (18.8 mm³/min), which was 62%

higher than that of EDA milling with a large cutting depth (11.6 mm³/min). Conventional ED milling showed the lowest MRR (1.97 mm³/min), failing to meet the requirements of efficient machining.

The new energy (chemical oxidation energy) released from the combustion of materials was used in the two types of EDA milling. Thus, the MRR of EDA milling was much higher than that of ED milling, which only relied on pulse power energy.

According to the analysis in Section 3.1, the short-circuit rate of EDA milling with a microcutting depth was only 2% because of the microcutting depth and short-circuit self-recovery. Thus, the probability of normal discharge was increased, and machining efficiency was improved. Meanwhile, the discharge combustion area of EDA milling with a large cutting depth was mainly in front of the electrode along the feeding direction (Fig. 10a). Most aerosol media flowed from the opposite direction of electrode feeding because of the blocking effect of the workpiece in this area, resulting in a significant reduction in oxygen passing through the combustion area and a corresponding reduction in ablation efficiency. The discharge combustion area of EDA milling with a microcutting depth was concentrated at the bottom of the electrode (Fig. 10b). The mixed aerosol medium with oxygen almost entirely flowed through the combustion area, and oxygen was fully used. Consequently, the MRR of EDA milling with a

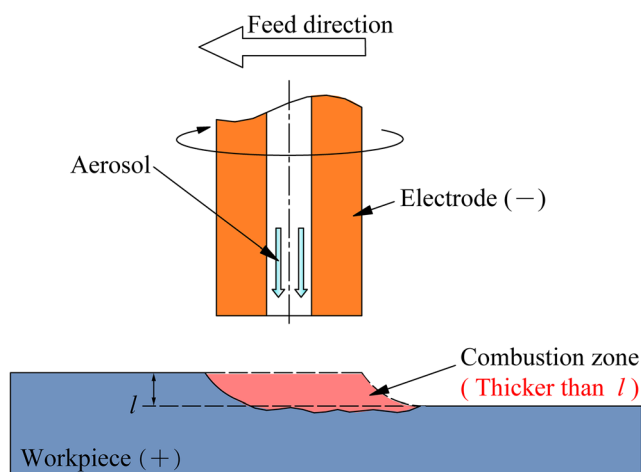


Fig. 5 Relationship between the thickness of ablated material and the cutting depth of single-layer l

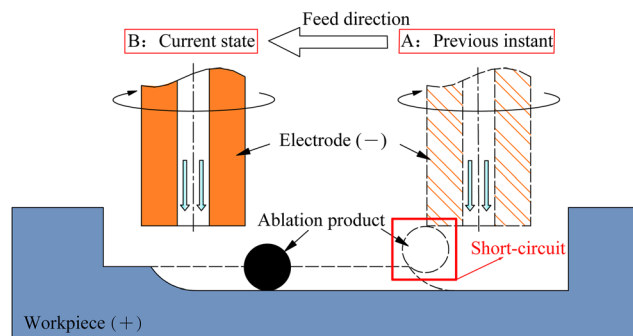


Fig. 6 Schematic of short-circuit self-recovery

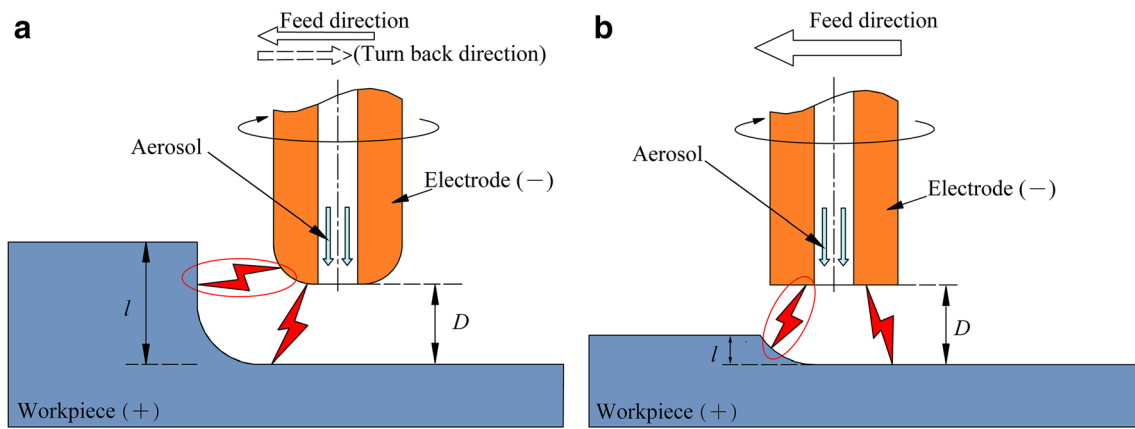


Fig. 7 Schematic of the discharge position. **a** EDA milling with a large cutting depth. **b** EDA milling with a microcutting depth

microcutting depth was 1.6 times higher than that of EDA milling with a large cutting depth.

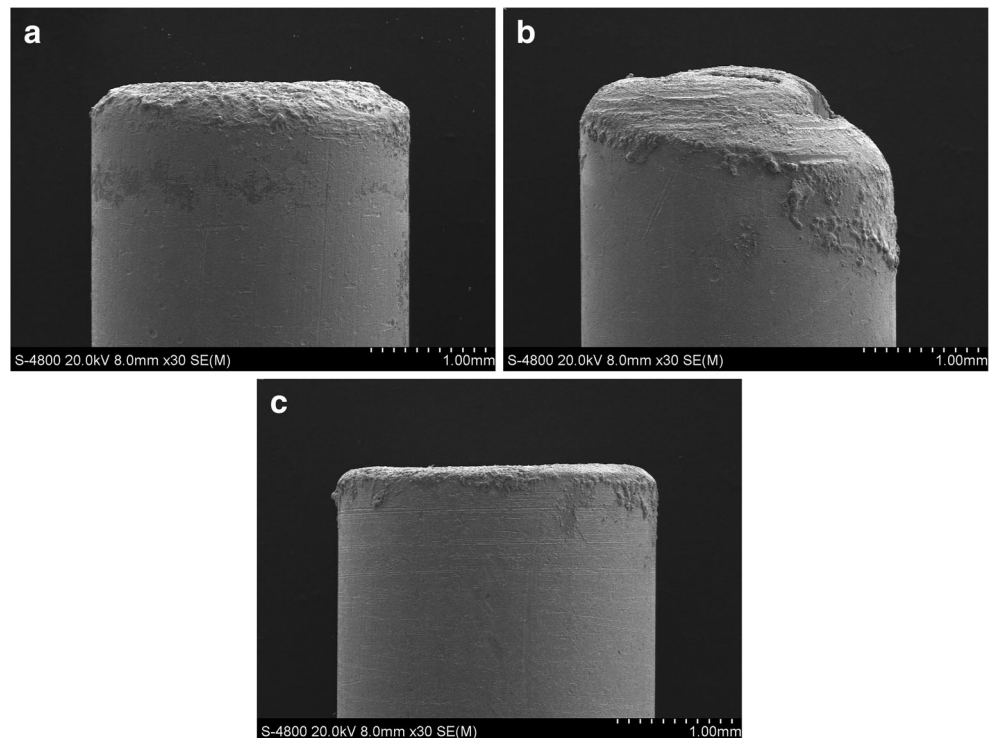
4.2 Analysis of RTWR

ED milling showed the highest RTWR (Fig. 9), and both types of EDA milling exhibited almost equal RTWRs. Numerous metal materials melted under the large amount of energy produced by combustion oxidation reactions. The electrode was protected and compensated by a portion of the molten metal and product that could not be removed. Therefore, machining with ablation reaction exhibited a lower RTWR than that of ED milling.

4.3 Cross-section shape precision analysis of straight groove

The cross-section shapes of the straight groove machined using two types of EDA milling are presented in Fig. 11a and b. The shape precision achieved by EDA milling with a microcutting depth was markedly higher than that by EDA milling with a large cutting depth. As described in Section 3.3, EDA milling with a large cutting depth resulted in a relatively significant side tool wear; thus, the electrode discharge position on the edge showed large non-uniform loss and formed a rounded corner, affecting the shape precision of the workpiece. EDA milling with a microcutting depth resulted in tool wear main at the end of the electrode, which

Fig. 8 SEM diagram of the electrode shape obtained using three different methods. **a** Conventional ED milling. **b** EDA milling with a large cutting depth. **c** EDA milling with a microcutting depth (note: Shot after machining with a depth of 2 mm under the conditions listed in Table 1)



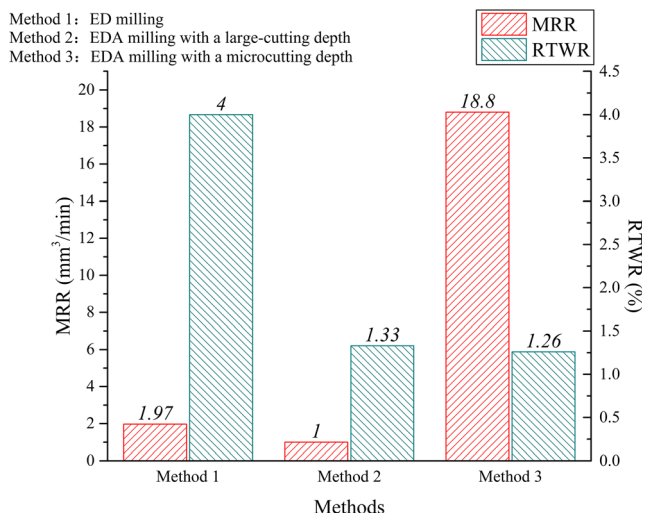


Fig. 9 MRR and RTWR under the three different methods

remained cylindrical. The shape precision of the machined groove was ensured.

4.4 Analysis of surface quality

The SEM image of the surface morphology of the bottom of the straight groove machined using the three methods are shown in Fig. 12. A large amount of metal was molten and removed from the machining area under the action of high-pressure aerosol medium under the two types EDA milling. The molten metal that was not promptly removed was cooled by the aerosol medium and solidified on the machined surface. EDA milling with a large cutting depth had a large cutting depth of the single layer. The electrode feed rate was low and stayed in one place for an extended time, allowing the molten metal to accumulate in the electrode discharge area and the re-solidified block to increase in size and thicken (Fig. 12a). EDA milling with a microcutting depth had a

microcutting depth of a single layer. The electrode feed speed was fast, and the heat source quickly left the ablation area. The molten metal was long and thin along the feed direction of the electrode, rendering the re-solidified block particularly thin and flaky (Fig. 12b).

Conventional ED milling relies on pulse power supply energy to remove materials. The machined surface had clear discharge pits and a small amount of re-solidified block (Fig. 12c).

Figure 13a presents the SEM image showing the surface morphology of the side of the straight groove machined by EDA milling with a large cutting depth. During processing, the discharge ablation reaction between the side of the electrode and the side wall resulted in a large number of re-solidified marks, and the size and thickness of the re-solidified block were greater than those of the bottom surface. The SEM image showing the surface morphology of the side of the straight groove machined by EDA milling with a microcutting depth is presented in Fig. 13b. During processing, no discharge ablation reaction occurred on the side wall, and the molten metal produced on the bottom surface passed through the side wall during removal and partly re-solidified on the side wall. Therefore, some re-solidified marks were observed on the surface of the side wall, but they were substantially reduced relative to those of the bottom surface.

5 Conclusion

In this study, EDA milling with a microcutting depth was proposed. The cutting depth of a single layer was less than the discharge gap, and spark discharge mainly occurred at the end of the electrode. The machining performance achieved was examined and compared with ED milling and EDA milling with a large cutting depth. The following are the conclusions drawn from the results of the study.

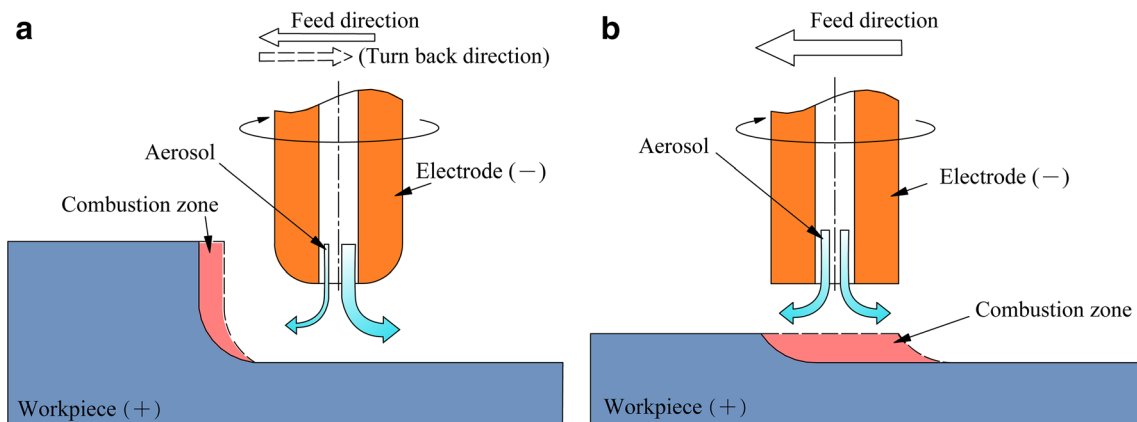


Fig. 10 Schematic of the aerosol medium flow direction and combustion area. a EDA milling with a large cutting depth. b EDA milling with a microcutting depth

Fig. 11 Comparison of the shape accuracy of the straight groove cross-section. **a** EDA milling with a large cutting depth. **b** EDA milling with a microcutting depth

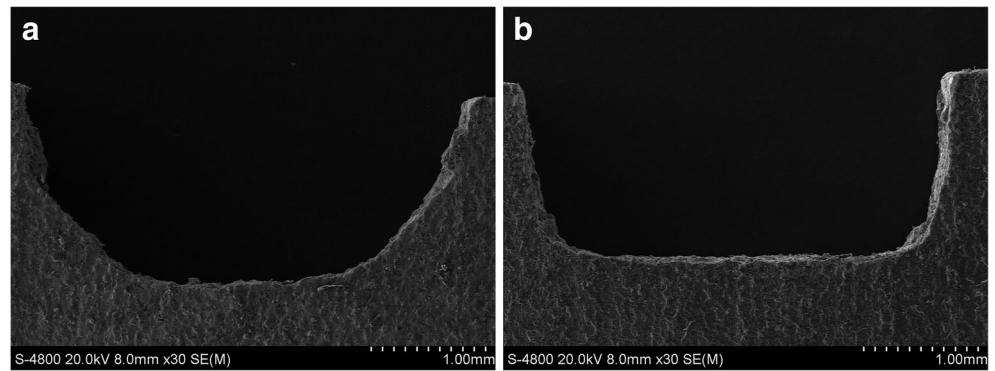


Fig. 12 SEM diagram of the bottoms of straight groove obtained using three different methods. **a** EDA milling with a large cutting depth. **b** EDA milling with a microcutting depth. **c** Conventional ED milling

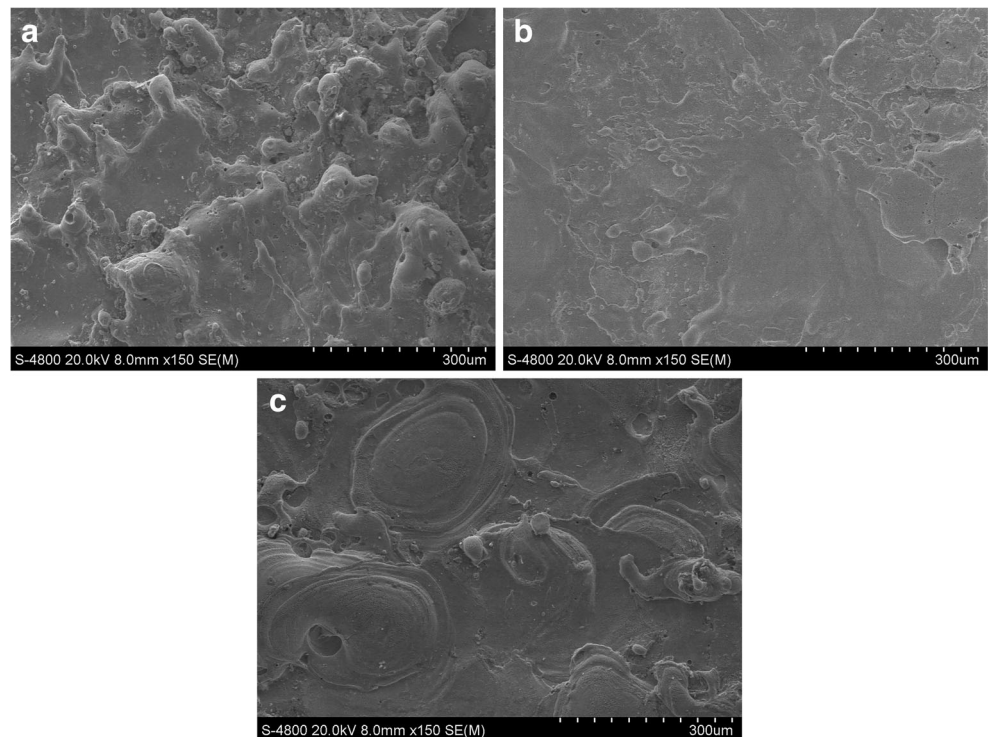
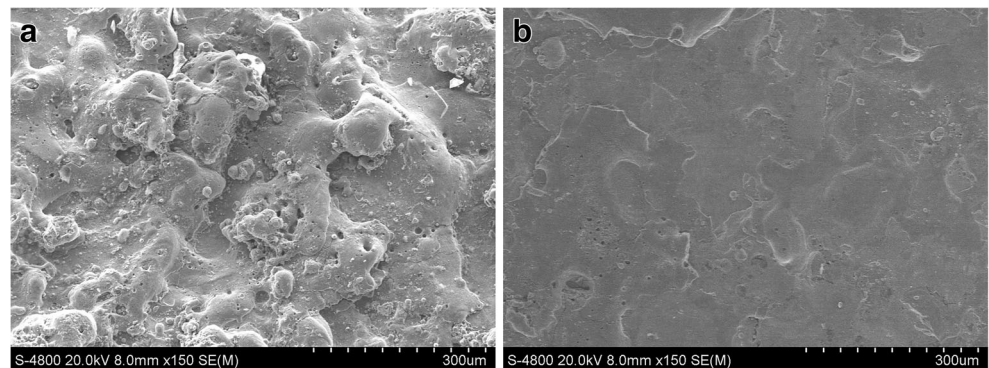


Fig. 13 SEM diagram of the side wall of straight groove obtained using three different methods. **a** EDA milling with a large cutting depth. **b** EDA milling with a microcutting depth



- (1) The machining state of the proposed method included normal discharge, short circuit, and open circuit. The short-circuit rate was considerably reduced because of the microcutting depth and short-circuit self-recovery, which improved the probability of normal discharge.
- (2) Under the same experimental conditions, the MRR of the proposed method ($18.8 \text{ mm}^3/\text{min}$) was 9.5 times that of ED milling ($1.97 \text{ mm}^3/\text{min}$) and increased by 62% relative to that of EDA milling with a large cutting depth ($11.6 \text{ mm}^3/\text{min}$).
- (3) The RTWR of the proposed method (1.26%) and EDA milling with a large cutting depth (1.33%) were almost the same.
- (4) The tool wear of the proposed method was axial loss, and the shape of the electrode remained cylindrical. The cross-section shape precision of the processed straight groove was significantly improved.
- (5) The proposed method is a high-precision machining technology. The technique improved the shape accuracy of the workpiece while maintaining high efficiency.

Acknowledgments The authors extend their sincere thanks to those who contributed in the preparation of the instructions.

Authors' contributions All authors have been personally and actively involved in substantive work leading to the report.

Funding This work is supported by the Postgraduate Research & Practice Innovation Program of Jiangsu Province (Grant Number KYCX18_0254) and National Natural Science Foundation of China (Grant Number 51975290).

Data availability The data and material set supporting the results are included within the article.

Declarations

Ethics approval and consent to participate Not applicable.

Consent for publication Not applicable.

Conflict of interest The authors declare no conflict of interest.

Code availability Not applicable.

References

1. Ho KH, Newman ST (2003) State of the art electrical discharge machining (EDM). *Int J Mach Tools Manuf* 43(13):1287–1300
2. Nikalje AM, Kumar A, Srinadh KVS (2013) Influence of parameters and optimization of EDM performance measures on MDN 300 steel using Taguchi method. *Int J Adv Manuf Technol* 69:41–49
3. Pham DT, Dimov SS, Bigot S, Ivanov A, Popov K (2004) Micro-EDM—recent developments and research issues. *J Mater Process Technol* 149(1-3):50–57
4. Mohri N, Suzuki M, Furuya M, Saito N, Kobayashi A (1995) Electrode wear process in electrical discharge machinings. *CIRP Ann* 44(1):165–168
5. Kunieda M, Kobayashi T (2004) Clarifying mechanism of determining tool electrode wear ratio in EDM using spectroscopic measurement of vapor density. *J Mater Process Technol* 149(1-3):284–288
6. Cheong HG, Kim YS, Chu CN (2019) Effect of reverse current on tool wear in micro-electrical discharge milling. *Precis Eng* 55:484–490
7. Wang J, Yang F, Qian J, Reynaerts D (2016) Study of alternating current flow in micro-EDM through real-time pulse counting. *J Mater Process Technol* 231:179–188
8. Bissacco G, Tristo G, Hansen HN, Valentincic J (2013) Reliability of electrode wear compensation based on material removal per discharge in micro EDM milling. *CIRP Ann* 62:179–182
9. Zarepour H, Tehrani AF, Karimi D, Amini S (2007) Statistical analysis on electrode wear in EDM of tool steel DIN 1.2714 used in forging dies. *J Mater Process Technol* 187-188:711–714
10. Zhang L, Du J, Zhuang X, Wang Z, Pei J (2015) Geometric prediction of conic tool in micro-EDM milling with fix-length compensation using simulation. *Int J Mach Tools Manuf* 89:86–94
11. Pei J, Zhang L, Du J, Zhuang X, Zhou Z, Wu S, Zhu Y (2017) A model of tool wear in electrical discharge machining process based on electromagnetic theory. *Int J Mach Tools Manuf* 117:31–41
12. Bleys P, Kruth J-P, Lauwers B, Zryd A, Delpretti R, Tricarico C (2002) Real-time tool wear compensation in milling EDM. *CIRP Ann* 51(1):157–160
13. Bleys P, Kruth J-P, Lauwers B (2004) Sensing and compensation of tool wear in milling EDM. *J Mater Process Technol* 149(1-3):139–146
14. Bellotti M, De Eguilior Caballero JR, Qian J, Reynaerts D (2021) Effects of partial tool engagement in micro-EDM milling and adaptive tool wear compensation strategy for efficient milling of inclined surfaces. *J Mater Process Technol* 288:116852
15. Yu ZY, Masuzawa T, Fujino M (1998) Micro-EDM for three-dimensional cavities - development of uniform wear method. *CIRP Ann* 47(1):169–172
16. Yu H-L, Luan J-J, Li J-Z, Zhang Y-S, Yu Z-Y, Guo D-M (2010) A new electrode wear compensation method for improving performance in 3D micro EDM milling. *J Micromech Microeng* 20(5):055011
17. Liang W, Tong H, Li Y, Li B (2019) Tool electrode wear compensation in block divided EDM process for improving accuracy of diffuser shaped film cooling holes. *Int J Adv Manuf Technol* 103:1759–1767
18. Li Z, Bai J, Zhu X (2016) Research on the depth error in micro electrical discharge milling. *Procedia CIRP* 42:638–643
19. Wang F, Liu Y, Zhang Y, Tang Z, Ji R, Zheng C (2014) Compound machining of titanium alloy by super high speed EDM milling and arc machining. *J Mater Process Technol* 214(3):531–538
20. Zhao W, Gu L, Xu H, Li L, Xiang X (2013) A novel high efficiency electrical erosion process - blasting erosion arc machining. *Procedia CIRP* 6:621–625
21. Wang X, Liu Z, Qiu M, Hui Z, Tian Z, Huang Y (2014) Mechanism of electrical discharge machining ablation. *Mater Manuf Process* 29(11-12):1367–1373
22. Han Y, Liu Z, Cao Z, Kong L, Qiu M (2018) Mechanism study of the combined process of electrical discharge machining ablation and electrochemical machining in aerosol dielectric. *J Mater Process Technol* 254:221–228

Publisher's note Springer Nature remains neutral with regard to jurisdictional claims in published maps and institutional affiliations.